Probabilistic Calibration of a Damage Rock Mechanics Model

Zenon Medina-Cetina, PhD, MSc, ME

Zachry Department of Civil Engineering, Texas A&M University, College Station TX, USA

Chloé Arson, PhD, MSc

School of Civil and Environmental Engineering, Georgia Institute of Technology, Atlanta GA, USA

Abstract.

Current practice in the calibration of damage models requires downscaling the effects of experimental observations from macro/meso to micro. This process introduces uncertainty that is seldom quantified to reflect the expert's confidence in the model predictions. A probabilistic calibration methodology can be introduced to overcome this problem. This paper shows a case study based on a damage rock mechanics model and triaxial experimental data on sandstone, where this approach is implemented to illustrate the impact of varying states of evidence (i.e. model complexity, experimental observations and expert's judgment) on the model predictions. Herein, the probabilistic calibration method relies on the use of the Bayesian paradigm to assimilate experimental observations into the probabilistic definition of the model parameters. Results of this approach can be encapsulated into a single probability distribution or *posterior*, which is later used to *assess the model performance*. The proposed approach shows the potential to improve current practice in risk analysis, since it allows to tracing changes of the model performance for varying evidence conditions in damage-sensitive geo-structures, such as nuclear waste disposals, landfills, geothermal wells and unconventional oil and gas formations, among others.

Rock; Damage Geomechanics, Probabilistic Calibration; Bayesian Paradigm; Uncertainty Quantification; Decision-Making

INTRODUCTION

One of the major challenges for the implementation of a geomechanical model is the proper characterization of its parameters. Nevertheless, it is common practice to ignore some or all the effects that *evidence* variability has on the model calibration resulting in a deterministic selection of model parameters. This implies that common sources of uncertainty may have little or no impact on the selection of the model parameters. In fact, two of the most frequent assumptions in the calibration of geomechanical parameters reflect the belief that there is only one combination of the constitutive parameters that can generate model predictions that best approximate the available experimental

observations (e.g. least-squares approach); and that the experimental data used for the model calibration belongs to a deterministic process. These assumptions are exacerbated in the case of geomechanical models used to simulate multiphysics and multiscale material behaviour (such as damage phenomena and thermo-hydro-mechanical-chemical couplings). That is, a large number of likely combinations of parameter estimates may yield similar model predictions, which may fit a single set of observations: the calibration of an advanced geomechanical model is ill-posed.

This problem is overcome by the use of a probabilistic calibration approach that can sample systematically likely combinations of the model parameters (Robert, 2007). Moreover, when using the Bayesian paradigm, it is possible to account for the influence of varying states of evidence (i.e. model complexity, experimental observations and expert's judgment), and to quantify any changes in the state of uncertainty.

The Bayesian approach has been used to calibrate numerous geomechanical models, such as liquefaction (Cetin et al., 2002), snow avalanches (Gauer et al., 2009), landslides (Ranalli et al., 2009 and 2013), tsunamigenic rockslides (Eidsvig et al., 2009), mudslides (Medina-Cetina and Cepeda, 2012), soils' constitutive models (Medina-Cetina, 2006; Medina-Cetina and Rechenmacher, 2009), foundations (You O.K. et al., 2011; Briaud et al., 2011), and more recently multiphysics geophysical inversions (Medina-Cetina et al., 2013), and probabilistic damage prediction in rocks (Arson and Medina-Cetina, 2013). However, the Bayesian paradigm has never been used to maximize damage model performance. The purpose of this work is to introduce a methodology that can be easily extended to a broader decision-making process, requiring the definition of optimal experimental settings and optimal geomechanical model formulations.

This paper introduces the probabilistic calibration of a damage model capable of simulating the evolution of the excavation damaged zone under thermo-hydro-mechanical geological conditions (Arson and Gatmiri 2009, 2010). Here, the damaged stiffness tensor is computed by applying the Principle of Equivalent Elastic Energy. Irreversible deformation induced by residual crack openings is related to damage, and the concept of equivalent stress state is introduced to reduce the number of thermodynamic postulates needed to close the formulation (Swoboda and Yang, 1999; Arson and Gatmiri, 2010).

An uncertainty quantification analysis is conducted assuming two scenarios: a) no availability of experimental observations and b) some availability of experimental observations. The latter is based on a triaxial compression test performed on dry sandstone (Dragon et al., 2000). This represents a simple case study, to illustrate the potential of the probabilistic calibration method to reproduce common conditions of exploratory model performance and standard calibration of constitutive parameters.

PROBABILISTIC CALIBRATION

The probabilistic calibration approach is defined within an uncertainty quantification framework UQ. The basis of this UQ framework is founded on the definition of a 'true process' vector $\mathbf{d}$, which in general represents values of observable variables (e.g., deformation, temperature, pore water pressure, crack density). Notice that in typical geomechanical problems or processes, $\mathbf{d}$ 'is not known a-priori'. However, if the true process is assumed to be random, $\mathbf{d}$ can be defined as a vector of random variables. On the other hand, what the modeller can determine are: (1) a vector of physical observations $\mathbf{d}_{obs}$, and (2) a vector of model predictions $\mathbf{d}_{pred}$ (prescribed at the same control points in space and time). Physical random deviations between $\mathbf{d}$ and $\mathbf{d}_{obs}$ and between $\mathbf{d}$ and $\mathbf{d}_{pred}$ can be simply expressed in the form of a vector $\Delta\mathbf{d}_{obs}$ and $\Delta\mathbf{d}_{pred}$ respectively (Medina-Cetina, 2006):

$$\mathbf{d} = \mathbf{d}_{obs} + \Delta\mathbf{d}_{obs} \tag{1}$$

$$\mathbf{d} = \mathbf{d}_{pred} + \Delta\mathbf{d}_{pred} = g\left(\boldsymbol{\theta}\right) + \Delta\mathbf{d}_{pred} \tag{2}$$

where $\mathbf{d}_{pred}$ represents a vector of predictions stemmed from the forward model $g\left(\boldsymbol{\theta}\right)$, conditioned on a vector of control parameters $\boldsymbol{\theta}$, which represent the experimental geometry conditions, material properties, initial or boundary conditions, and even hyper-parameters such as statistics defining the likely variations of the experimental observations or the model predictions, or even the influence of the computational implementation. Similarly to the vector of the process response $\mathbf{d}$, $\boldsymbol{\theta}$ can be defined as the addition of a mean $\hat{\boldsymbol{\theta}}$ and a random component $\Delta\boldsymbol{\theta}$, such that:

$$\boldsymbol{\theta} = \hat{\boldsymbol{\theta}} + \Delta\boldsymbol{\theta} \tag{3}$$

As a result, four different scenarios can be generated after combining the potential sources of uncertainty (Medina-Cetina, 2006). These can be generalized from the most uncertain scenario represented by $\left\{\Delta\mathbf{d}_{obs} - \Delta\mathbf{d}_{pred}\right\} = \left[\mathbf{d}_{pred} - \mathbf{d}_{obs}\right]$, which can be defined by a single uncertainty metric $\Delta\mathbf{d} = \left[\mathbf{d}_{pred} - \mathbf{d}_{obs}\right]$. Notice that this latter formulation is typically used in deterministic calibrations such as least-squares for the back-calculation of model parameters (Benjamin and Cornell, 1970), which is only valid when the model predictions are unbiased along the domain of interest (where $\mathbf{d}$ is defined). That is, when the probabilistic expectation of $E\left[\Delta\mathbf{d}_{obs} - \Delta\mathbf{d}_{pred}\right] = 0$.

In this work, the probabilistic calibration consists in mapping the deformation of a rock sample during a triaxial test ($\mathbf{d}_{obs}$) onto the damage model's governing parameters ($\boldsymbol{\theta}$). The Bayesian paradigm formulates the probabilistic solution to the inverse problem as (Robert, 2007):

$$\pi\left(\boldsymbol{\theta}\middle|\mathbf{d}_{obs}\right) = \frac{f\left(\mathbf{d}_{obs}\middle|\boldsymbol{\theta}, \mathrm{g}\left(\boldsymbol{\theta}\right)\right)\cdot\pi\left(\boldsymbol{\theta}\right)}{\int f\left(\mathbf{d}_{obs}\middle|\boldsymbol{\theta}, \mathrm{g}\left(\boldsymbol{\theta}\right)\right)\cdot\pi\left(\boldsymbol{\theta}\right)\cdot \mathrm{d}\boldsymbol{\theta}} \tag{4}$$

where $\pi\left(\boldsymbol{\theta}\right)$ is the prior probability distribution of the model parameters encapsulating the current knowledge about the random nature of $\boldsymbol{\theta}$; $f\left(\mathbf{d}_{obs}\middle|\boldsymbol{\theta}, \mathrm{g}\left(\boldsymbol{\theta}\right)\right)$ is the likelihood probability density function, which defines a measure of the trade-off between the observations and the model predictions given a set of parameters $\boldsymbol{\theta}$; and $\pi\left(\boldsymbol{\theta}\middle|\mathbf{d}_{obs}\right)$ is the probabilistic solution to the inverse problem or posterior distribution. The computational implementation of this problem follows the Markov-Chain Monte-Carlo approach (Robert and Casella, 2004), and requires the setting of hypotheses on the shapes of the probability distributions for the prior and likelihood functions based on the expert's judgement.

The case study discussed in this work is based on a thermo-hydro-mechanical damage model formulated for unsaturated porous media in geological storage conditions (the "THHMD" model: Arson and Gatmiri, 2009, 2010). The damage variable here is the second-order crack density tensor (Kachanov, 1992), noted $\boldsymbol{\Omega}$. The THHMD model is formulated in independent strain state variables: mechanical strains ε_M, capillary strains ε_{Sv} and thermal strains ε_{Tv}, which respectively conjugate to

net stress $\sigma'' = \sigma - p_a\delta$, suction $s = p_a - p_w$ and thermal stress p_T (in which p_w and p_a are the liquid water and gaseous air pore pressures, and δ is the second-order identity tensor). The stress/strain relationships are derived from the expression of Helmholtz free energy, which is postulated to be the sum of damaged deformation elastic energies and of potentials related to the existence of residual strains after unloading:

$$\psi_s\left(\varepsilon_M, \varepsilon_{Sv}, \varepsilon_{Tv}, \mathbf{\Omega}\right) = \frac{1}{2}\varepsilon_M : \mathbf{D_e}\left(\mathbf{\Omega}\right) : \varepsilon_M + \frac{1}{2}\varepsilon_{Sv}\beta_s\left(\mathbf{\Omega}\right)\varepsilon_{Sv} + \frac{1}{2}\varepsilon_{Tv}\beta_T\left(\mathbf{\Omega}\right)\varepsilon_{Tv} - g_M\mathbf{\Omega} : \varepsilon_M - \frac{g_S}{3}Tr\left(\mathbf{\Omega}\right)\varepsilon_{Sv} - \frac{g_T}{3}Tr\left(\mathbf{\Omega}\right)\varepsilon_{Tv} \quad (5)$$

$\beta_s\left(\mathbf{\Omega}\right)-$ and $\beta_T\left(\mathbf{\Omega}\right)$ are the elastic capillary and thermal moduli, defined from the thermodynamic conjugation relationships: $s = \beta_s\left(\mathbf{\Omega}\right)\varepsilon_{Sv}^e$ and $p_T = \beta_T\left(\mathbf{\Omega}\right)\varepsilon_{Tv}^e$. g_M, g_S and g_T are material parameters representing mechanical, capillary and thermal crack toughness. An associate damage flow rule is adopted. Damage is assumed to propagate under the influence of tensile mechanical, capillary or thermal stress, which are gathered into a unique variable, called the "damage driving force":

$$\mathbf{Y}_d = -\frac{\partial\psi_s}{\partial\mathbf{\Omega}}, \quad \mathbf{Y_{d1}} = g_M\varepsilon_M + g_S\varepsilon_{Sv} + g_T\varepsilon_{Tv}, \quad \mathbf{Y_{d1}^+} = g_M\varepsilon_M^+ + g_S\varepsilon_{Sv}^- + g_T\varepsilon_{Tv}^+ \quad (6)$$

To illustrate the applicability of the proposed method, a simple case study is defined. A first scenario assumes the absence of experimental observations, accounting only for the expert's judgement (Case I). Notice that this condition is typical of exploratory model behaviour. Here, based on expert's judgement, probability density functions for the prior of both mechanical and damage parameters are formulated, and then sampled independently using a standard Monte Carlo approach, to generate varying model predictions (an alternative approach would be to use well-known correlations from similar materials, but in that case a 'hyper-parameter' would be required to describe the extent or strength of the unknown correlation). A second scenario makes use of the previous prior distributions, and of newly introduced experimental data, which defines the formulation of a likelihood function. This allows for conducting the probabilistic calibration yielding a posterior probability distribution (Case II).

In Case II, results of triaxial compression tests performed on dry sandstone under a confining pressure of p_c=15MPa (Dragon et al., 2000) are used as prior. For simplicity, only Young's modulus E and the damage parameter g_M were defined as the control random parameters. In Case I, the vector of random parameters was $\boldsymbol{\theta} = \{E,\ g_M\}$, where the mean of E (1.17x10^{10} Pa) and the mean of g_M (-3.2 x10^7 Pa) were defined from limited experimental data (Dragon et al., 2000). E and g_M were assumed to follow a lognormal distribution and an inverse exponential distribution, respectively (for both E and g_M: CoV=0.1). Figure 1a shows a probability map representing the independent sampling of combinations of E and g_M, and Figure 1b shows a set of simulations of the damage model predictions, with the experimental data on the background as a reference (4,000 realizations of the material's stress-strain response).

Case II introduces the vector of observed data $\mathbf{d_{obs}}$. The likelihood is defined as a varying independent Gaussian distribution around the experimental observations, with mean equal to the experimental strain-stress values. Based on soil triaxial tests performed on independent samples under similar experimental conditions (Medina-Cetina and Rechenmacher, 2009), variance is assumed to vary as a linear function of the deviator stress (CoV=0.05). This estimate is suggested to define an uncertainty band around the experimental stress-strain curve, which can help to select of reject a set of model parameters proposed for fitting the experimental observations. In a more comprehensive study, the CoV can be defined as a hyper-parameter, and be included as part of the vector of random parameters $\boldsymbol{\theta}$. Figures 2 a-d present results of the resulting probabilistic calibration. The cumulative density functions CDF of E and g_M (Fig. 2.a and 2.b respectively) show a significant reduction on the uncertainty for both parameters after the inclusion of the experimental evidence. This is summarized by the joint probability map between E and g_M (Fig. 2.c), where a distinct correlation is observed with a correlation coefficient ρ=0.3. This map is comparable with figure 1.a of Case I, where there was no notion of any correlation between parameters. A sample of model responses (4,000 realizations) with the corresponding observations in the background is presented (Fig. 2.d), which further reassures the impact of adding evidence into the probabilistic calibration process when compared to figure 1.b.

Results from Case II show that larger mechanical tensile strains $\varepsilon_{\mathbf{M}}^{+}$ (in the radial directions) are expected for lower Young's moduli. Under similar loading conditions, decreased elastic moduli increase indeed $\varepsilon_{\mathbf{M}}^{+}$, and therefore the damage-driving force (Equation 6). In order to maintain the same damage-driving force (so as to predict the observed mount of damage), g_M should decrease when $\varepsilon_{\mathbf{M}}^{+}$ increases. As a result, low values of E are correlated to high absolute values of g_M. The joint probability map obtained with prior observation data (Figure 2.c) highlights this correlation. In the elastic domain and for a given state of stress, $\varepsilon_{\mathbf{M}}^{+}$ increases linearly with $1/E$. For a given prediction on $\mathbf{Y}_{\mathbf{d1}}^{+}$, the absolute value of $1/g_M$ depends linearly on $\varepsilon_{\mathbf{M}}^{+}$ (Equation 6). Therefore, the correlation between E and g_M is expected also to be linear.

The model performance is finally measured by computing the mean and standard deviation of the expected behaviour of the process evaluated from the model predictions on Cases I and II (Figures 3.a. and 3.b respectively). The means show that on both evidence conditions the model is capable of matching the experimental observations. It is worth noticing that although the last few experimental observations seem a bit shifted from the model predictions, this is because the model in many cases shows brittle failure before the experimental observations, meaning that statistics about the mean at the end of the stress-strain response are affected by the varying number of available model predictions. On the other hand, a significant difference is found for the standard deviations: the deviation between the two states of evidence grows with the specimen deformation, reaching a maximum difference of the order of 5 times at about $\varepsilon_z = 0.01$. Which provide a comparison metric that can serve as a reference for further interventions in the modelling when new data from additional physics are included, and when the model complexity is increased to resemble these new experimental conditions.

CONCLUSIONS

A probabilistic approach is proposed to assess the predictive performance of a damage rock mechanics model. A probabilistic calibration was performed with no experimental data (Case I), and with results from one single experimental test (Case II). Two material parameters were defined as random variables (Young's modulus *E* and damage parameter g_M). The posterior generated in Case II showed first and

second order statistics for E and g_M (as opposed to deterministic calibrations which only provide a single vector of parameters), from which the model performance was conducted. A comparison of the model predictions between these two cases demonstrates a significant reduction of the uncertainty on the model predictions from Case I to Case II. The theoretical framework presented in this paper is expected to facilitate and improve the reliability and performance assessment of multiphysics and multiscale damage models, due its ability to quantify the state of uncertainty for varying states of evidence availability.

REFERENCES

Arson C. and Gatmiri B. (2009). "A mixed damage model for unsaturated porous media." *Comptes-Rendus de l'Académie des Sciences de Paris, section Mécanique* **337**, 68-74.

Arson C. and Gatmiri B. (2010). "Numerical study of a thermo-hydro-mechanical model for unsaturated porous media." *Annals of Solid and Structural Mechanics* **1 (2)**, 59-78.

Arson C. and Medina-Cetina Z. (2013 - under review). "Bayesian Paradigm to Assess Rock Compression Damage Models." *Environmental Geotechnics.*

Benjamin, J.R. and C.A. Cornell (1970), "Probability, Statistics, and Decision for Civil Engineers," McGraw-Hill.

Briaud J.L. Medina-Cetina Z., Everett M., Hurlebaus S., Yousefpour N., Arjwech R., Tucker S (2011). "Unknown Foundation Determination for Scour," Texas Department of Transportation, Report No. 0-6604.

Cetin K. O., Kiureghian A.D., Seed R.B. (2002) "Probabilistic models for the initiation of seismic soil liquefaction," *Structural Safety* **24 (1)**, 67–82.

Dragon, A., Halm, D. and Désoyer, T. (2000). "Anisotropic damage in quasi-brittle solids : modelling, computational issues and applications." *Computer Methods in Applied Mechanics and Engineering* **183**, 331–352.

Eidsvig U.M., Medina-Cetina Z., Kveldsvick V., Glimsdal S., Harbitz C.B., Sandersen F. (2009) "Risk Assessment of a Tsunamigenic Rockslide at Aknes", Natural Hazards: Special Issue of '40th anniversary of the Research Society INTERPRAEVENT' **56 (2)**, 529 - 545

Gauer P., Medina-Cetina Z., Lied K. and Kristensen K. (2009), "Optimization and Probabilistic Calibration of Avalanche Block Models, "*Cold Regions Science and Technology* **59 (2-3)**, 251-258.

Kachanov, M. (1992). Effective elastic properties of cracked solids: critical review of some basic concepts". Applied Mechanics Reviews **45 (8)**, 304–335.

Medina-Cetina, Z. (2006), "Probabilistic Calibration of Soil Constitutive Models," Dissertation, Philosophy Doctor, The Johns Hopkins University, Baltimore MD, USA.

Medina-Cetina Z. and Cepeda J. (2012), "Probabilistic Classification of Local Rainfall-Thresholds for Landslide Triggering," *International Journal of Natural Disasters, Accidents and Civil Infrastructure* **12 (1)**, 76-83.

Medina-Cetina Z., Esmailzadeh S., Kang J.W. and Kallivokas L.F. (2013), "Bayesian Inversion of Heterogeneous Media: Introducing the Next Generation of Integrated Studies for Offshore Site Investigations," Offshore Technology Conference OTC, May 6-9 Houston TX.

Medina-Cetina Z. and Rechenmacher A.L. (2009), Influence of Boundary Conditions, Specimen Geometry and Material Heterogeneity on Model Calibration from Triaxial Tests. *International Journal for Numerical and Analytical Methods in Geomechanics* **34 (6)**, 627 – 643.

Ranalli M., Gottardi G., Medina-Cetina Z. and Nadim F. (2009), "Uncertainty Quantification in the Calibration of a Dynamic Visco-Plastic Model of Slow Slope Movements," *Landslides*, **7 (1)**, 31-41.

Ranalli M., Medina-Cetina Z., Gottardi G. and Nadim F. (2013), "Probabilistic Calibration of a Dynamic Model for Predicting Rainfall Controlled Landslides," ASCE's *Journal of Geotechnical and Geoenvironmental Engineering* : http://ascelibrary.org/doi/pdf/10.1061/%28ASCE%29GT.1943-5606.0000972 .

Robert C.P. (2007), The Bayesian Choice, Springer-Verlag NewYork, USA.

Robert C.P. and Casella G. (2004). Monte Carlo Statistical Methods. Springer, New York.

Swoboda, G. and Yang, Q. (1999). "An energy-based damage model of geomaterials 1. Formulation and numerical results." *International Journal of Solids and Structures* **36**, 1719–1734.

Yu O.K., Medina-Cetina Z. and Briaud J.L. (2011), "Towards an Uncertainty-Based Design of Foundations for Onshore Oil and Gas Environmentally Friendly Drilling (EFD) Systems," Proceedings of the Geo-Frontiers Conference, Dallas TX USA, March 13-16.

(a)	*(b)*

Fig. 1.
a. Probability map representing the independent sampling of combinations of E and g_M (sampling of light yellow nodes in Fig. 1.a). b. THHMD model predictions for a triaxial compression test on dry sandstone in Case I (experimental results are represented by bright green node in Fig. 1.b): in Case I, probability functions are defined based on expert's opinion, assuming that the experimental data used for model verification are not available a priori). $\sigma_{\mathbf{d}}$ *is the deviator stress:* $\sigma_{\mathbf{d}} = \sigma_z - \sigma_r = \sigma_z - p_c$.

(a)	*(b)*
(c)	*(d)*

Fig. 2.

Fig. 2.a and 2.b contrast the CDFs of E and g_M before (prior – Case I) and after (posterior – Case II) introducing experimental observations (notice the change in the range for each parameter). Fig. 2.c. presents the probability map of the probabilistic calibration of E and g_M in Case II. Fig. 4.d introduces the stress-strain THHMD model responses based on the sampling of the posterior given in Fig. 2.c (experimental observations plotted in the background).

(a)	*(b)*

Fig. 3.

a. Mean of model predictions from Case I (Prior) and Case II (Posterior) compared to available experimental observations. b. Standard deviations of the expected model predictions for Case I and Case II.

List of notation

$\mathbf{d}$ Vector of the 'true' process (unknown)

$\mathbf{d}_{obs}$ Vector of experimental observations

$\mathbf{d}_{pred}$ Vector of model predictions

$\Delta\mathbf{d}_{obs}$ Vector uncertainty measures related to the experimental observations

$\Delta\mathbf{d}_{pred}$ Vector uncertainty measures related to the model predictions

$g(\boldsymbol{\theta})$ Vector model predictions as a function of the vector of model parameters $\boldsymbol{\theta}$

$\hat{\boldsymbol{\theta}}$ Vector of mean estimates of the model parameters

$\Delta\boldsymbol{\theta}$ Vector of uncertainty measures related to the model parameters

$\Delta\mathbf{d}$ Vector of uncertainty measures related to both the experimental observations and the model parameters

$\pi(\boldsymbol{\theta})$ Prior probability distribution

$f\left(\mathbf{d}_{obs}\middle|\boldsymbol{\theta},\mathrm{g}(\boldsymbol{\theta})\right)$ Likelihood probability distribution

$\pi\left(\boldsymbol{\theta}\middle|\mathbf{d}_{obs}\right)$ Posterior probability distribution

$\boldsymbol{\Omega}$ Second-order crack density tensor

ε_M Mechanical strains

ε_{Sv} Capillary strains

ε_{Tv} Thermal strains

σ'' Net stress

σ Total stress

p_a Gaseous pressure

δ Second order identity tensor

s Suction

p_w Water pressure

p_T Thermal stress

$\beta_s(\boldsymbol{\Omega})-$ Elastic capillary moduli

$\beta_T(\boldsymbol{\Omega})$ Thermal moduli

g_M Material mechanical crack toughness

g_S	Material capillary crack toughness
g_S	Material thermal crack toughness
Ψ	Rock solid matrix's Helmholtz free energy
$\boldsymbol{Y}$	Energy release rate (to open cracks) / affinity
E	Rock Young's modulus
CoV	Coefficient of variation
ρ	Coefficient of correlation

Figure
Click here to download high resolution image

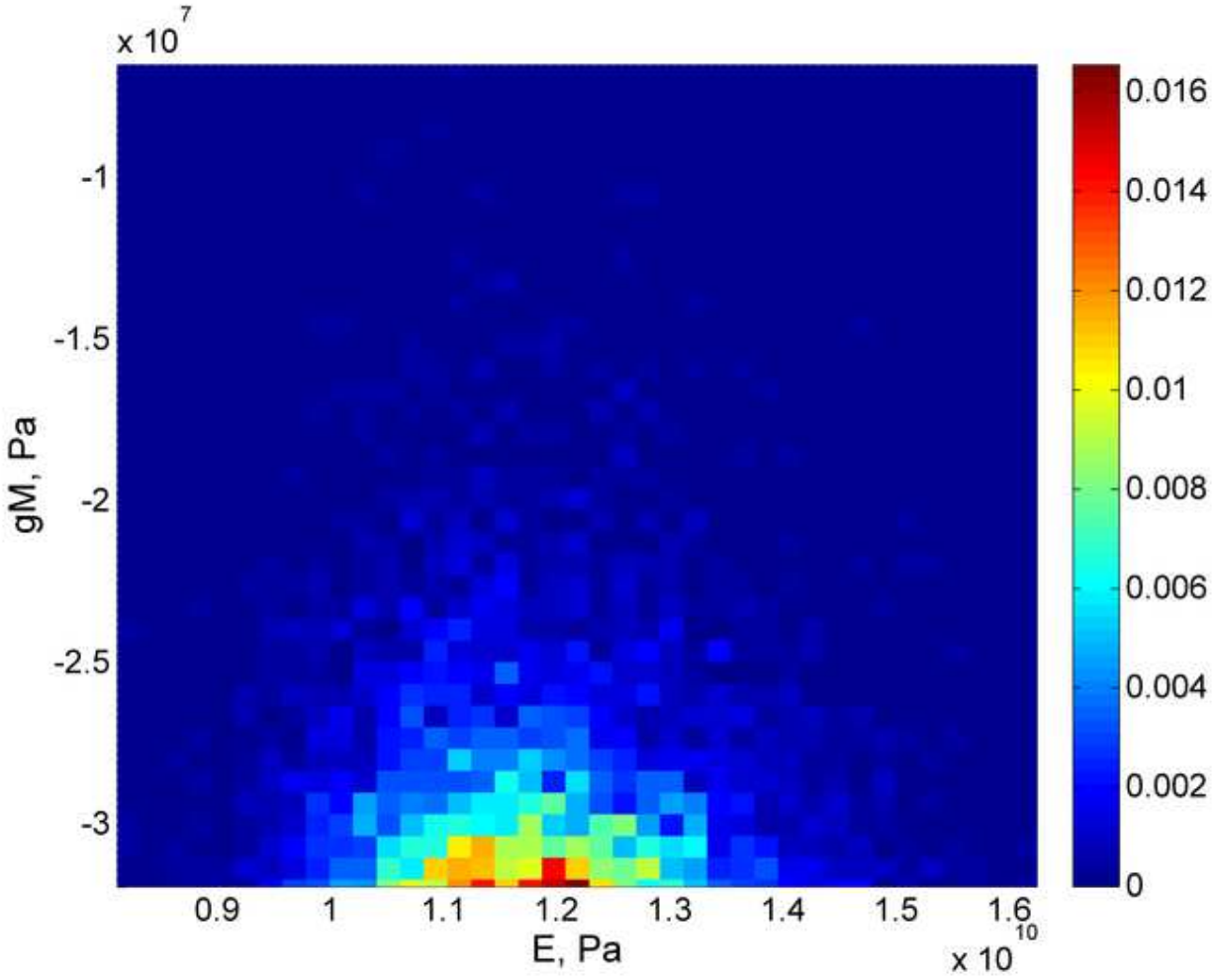

Figure
Click here to download high resolution image

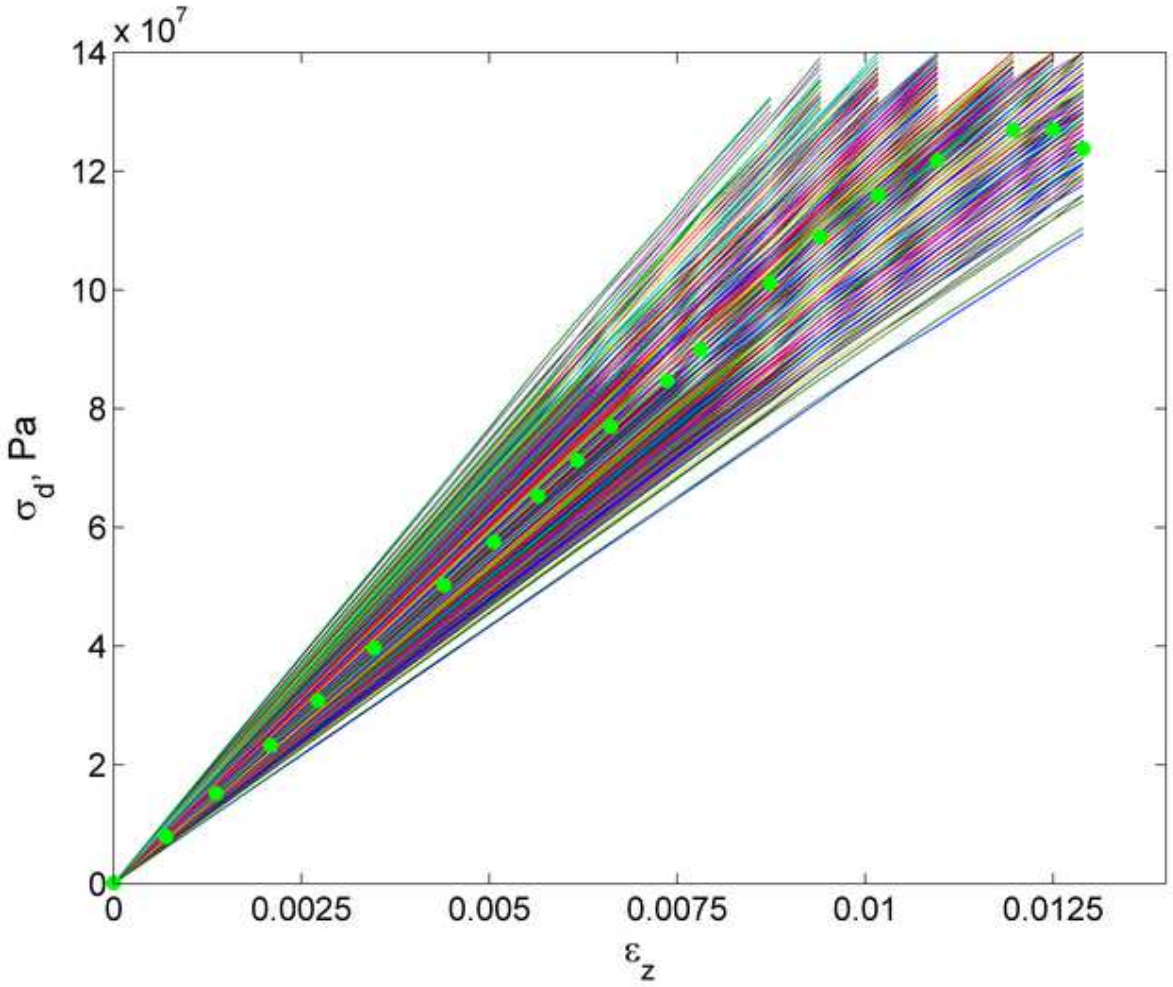

Figure
Click here to download high resolution image

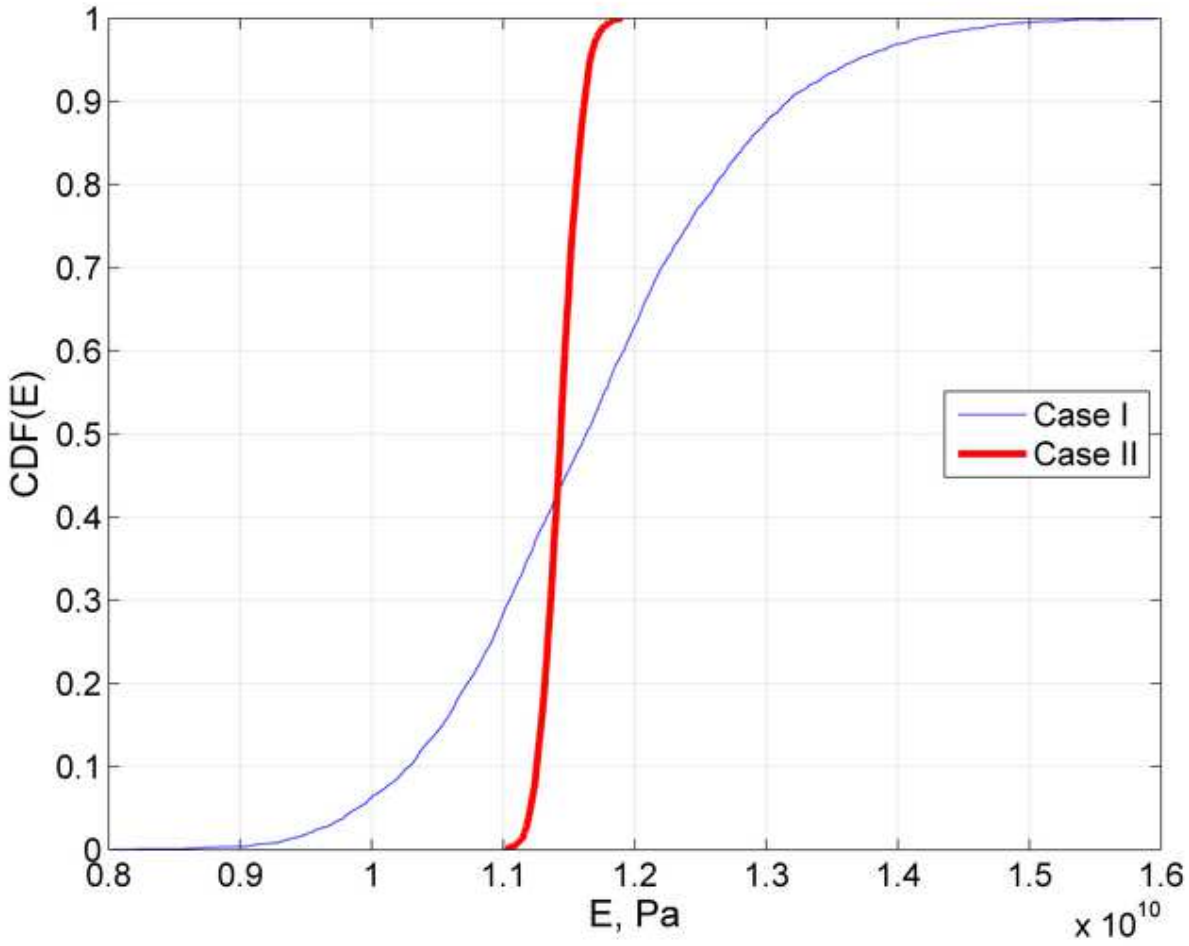

Figure
Click here to download high resolution image

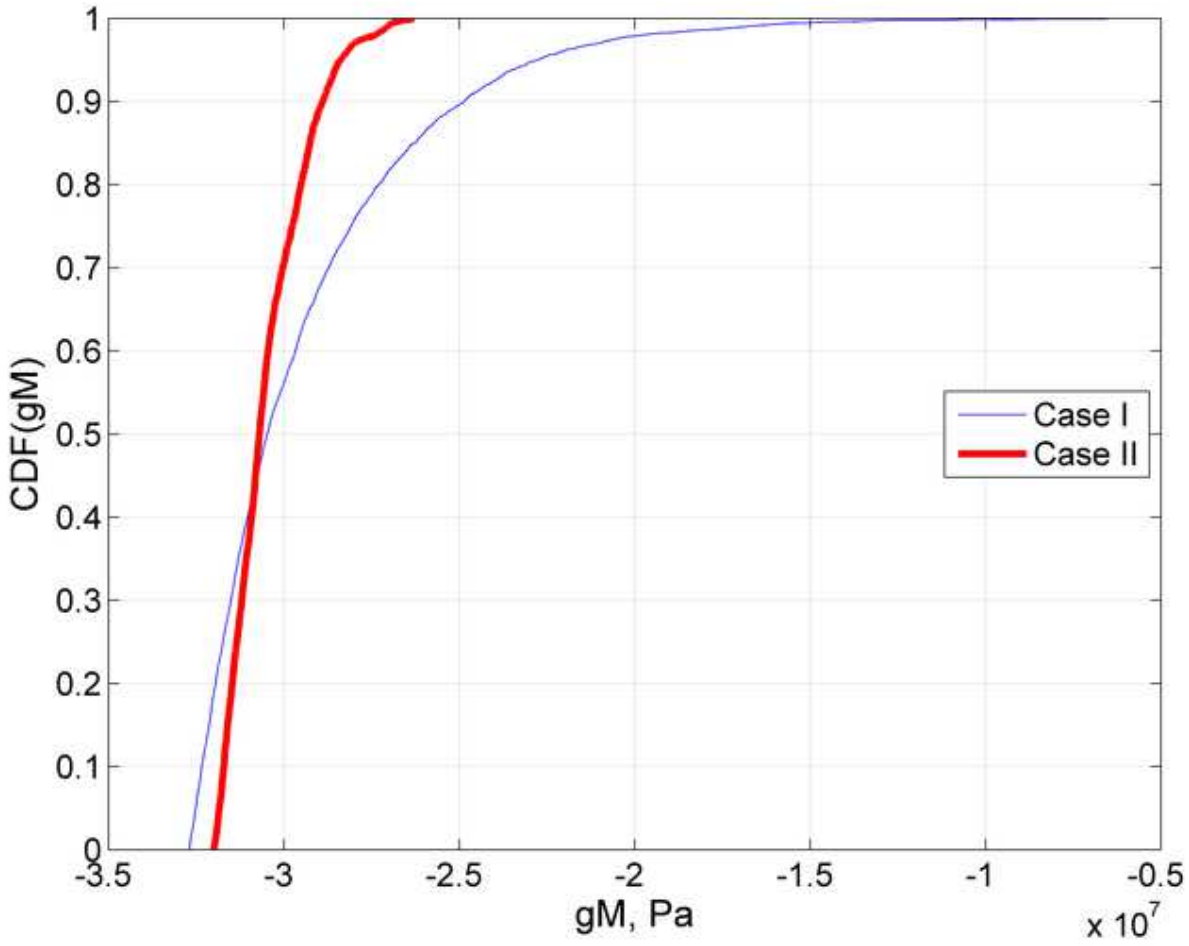

Figure
Click here to download high resolution image

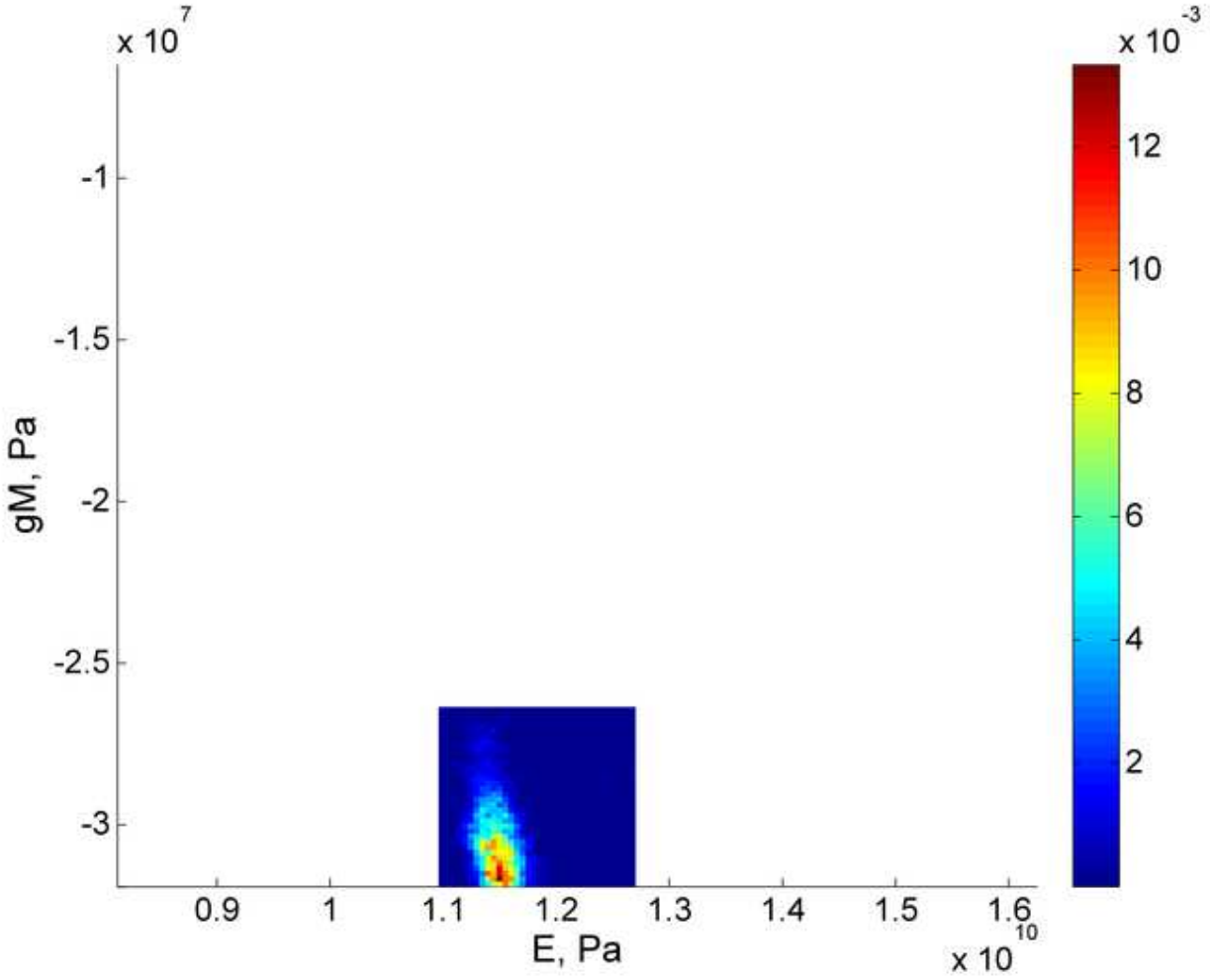

Figure
Click here to download high resolution image

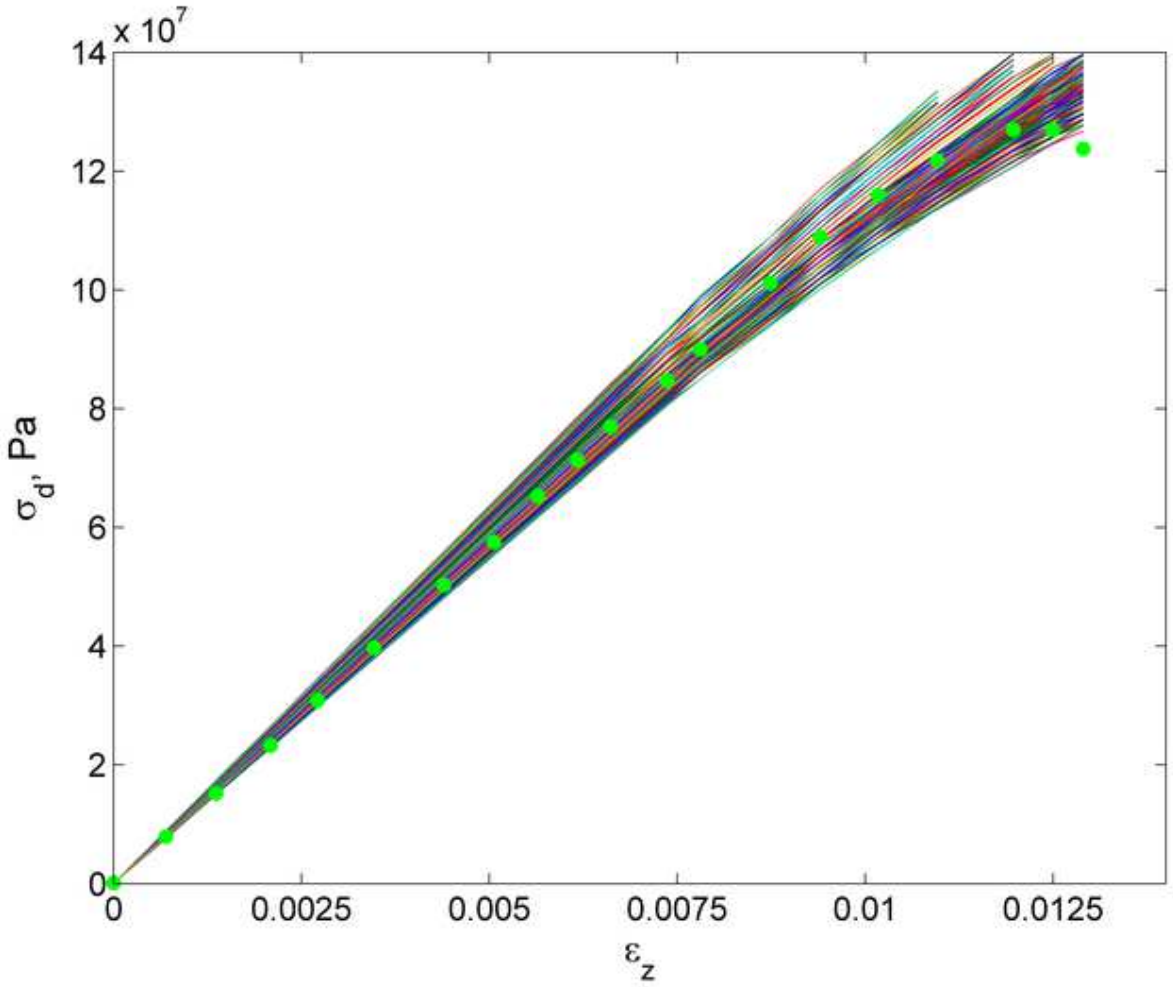

Figure
Click here to download high resolution image

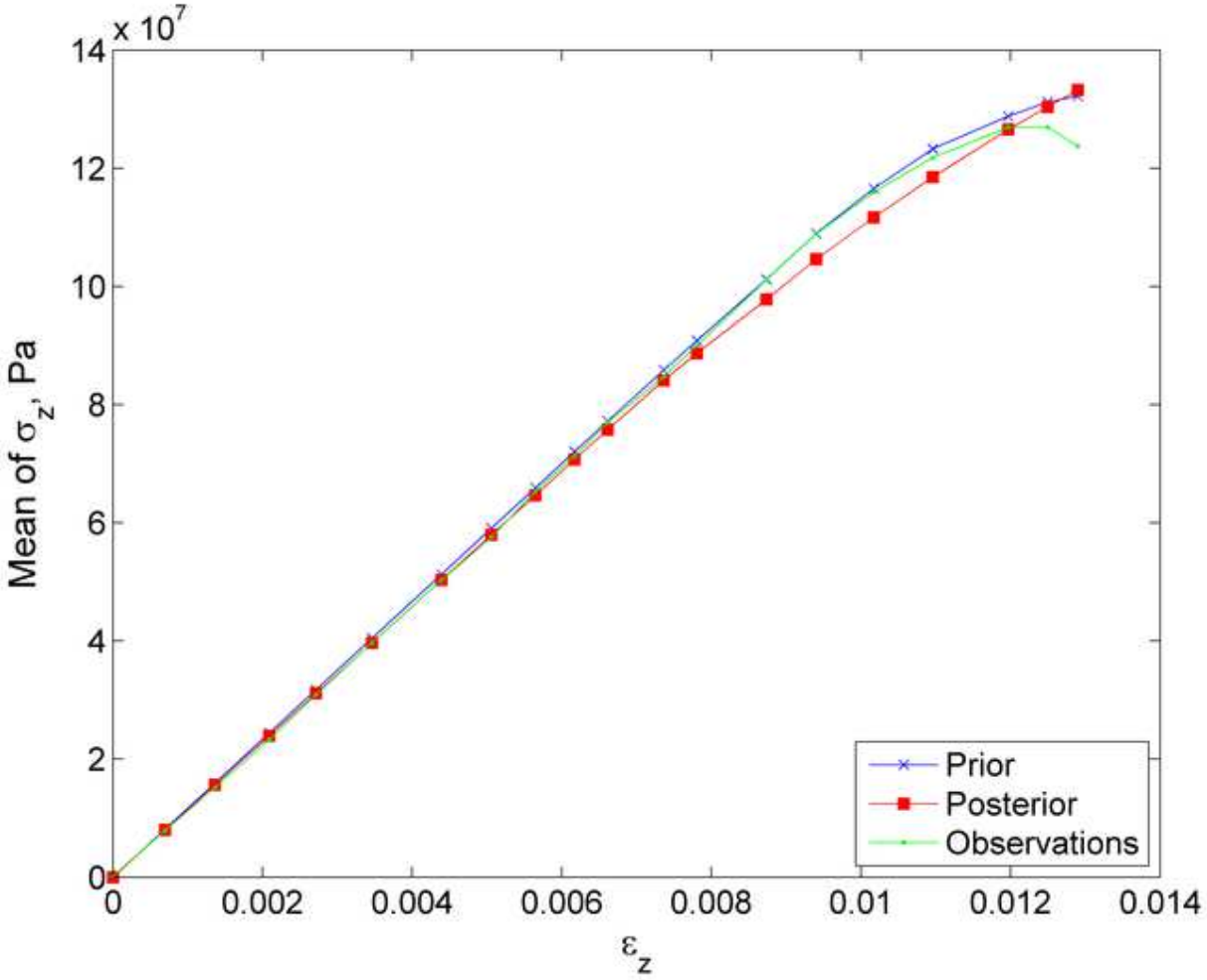

Figure
Click here to download high resolution image